ORGANIC LETTERS

2007
Vol. 9, No. 8
1481−1484

Blue-Colored Donor–Acceptor [2]Rotaxane

Taichi Ikeda, Ivan Aprahamian, and J. Fraser Stoddart*

California NanoSystems Institute, and Department of Chemistry and Biochemistry, University of California, Los Angeles, 405 Hilgard Avenue, Los Angeles, California 90095

stoddart@chem.ucla.edu

Received January 23, 2007

ABSTRACT

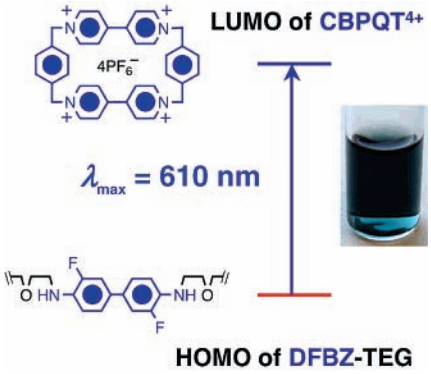

A guest molecule—a bis-*N*-tetraethyleneglycol-substituted 3,3′-difluorobenzidine derivative—has been synthesized, and its complexation with the host, cyclobis(paraquat-*p*-phenylene), has been investigated. This host–guest complex was then employed in the template-directed synthesis of a blue-colored [2]rotaxane. The color of this [2]rotaxane arises from the charge-transfer absorption band between the HOMO of the guest and the LUMO of the host. This host–guest complex, and the derived [2]rotaxane, completes the donor–acceptor-based RGB (red/green/blue) color complex set.

The discovery[1] of cation recognition by crown ethers has led to the design and synthesis of a myriad of host−guest systems employing hosts such as cyclodextrins,[2] calixarenes,[3] cucurbiturils,[4] etc. In addition to these hosts, the tetracationic cyclophane, cyclobis(paraquat-*p*-phenylene)[5] (**CBPQT**$^{4+}$), enjoys a unique stature in host−guest chemistry[6] on account of its insatiable appetite to bind π-electron-rich systems. The π-electron-poor CBPQT^{4+} ring interacts with π-electron-rich guest molecules by means of charge-transfer (CT) interactions, conferring useful electrochemical[7] and electrooptical[8] properties upon the host−guest system. The color of the complex with **CBPQT**$^{4+}$ as the host is determined by the wavelength of the CT absorption band,[5a,8,9] whereas the absorption wavelength depends on the energy gap between the LUMO of **CBPQT**$^{4+}$ and the HOMO of the guest molecule.[5a,9d] Thus, we can generate a range of different colors by altering the HOMO energy level of the guest

(1) (a) Pedersen, C. J. *Science* **1988**, *241*, 536−540. (b) Pedersen, C. J. *J. Am. Chem. Soc.* **1967**, *89*, 2495−2496.

(2) (a) Wenz, G.; Han, B.-H.; Mueller, A. *Chem. Rev.* **2006**, *106*, 782−817. (b) Harada, A. *Acc. Chem. Res.* **2001**, *34*, 456−464. (c) Nepogodiev, S. A.; Stoddart, J. F. *Chem. Rev.* **1998**, *98*, 1959−1976.

(3) (a) Menon, S. K.; Sewani, M. *Rev. Anal. Chem.* **2006**, *25*, 49−82. (b) Bohmer, V. *Angew. Chem., Int. Ed.* **1995**, *34*, 713−745. (c) Shinkai, S. *Tetrahedron* **1993**, *49*, 8933−8968.

(4) (a) Lagona, J.; Mukhopadhyay, P.; Chakrabarti, S.; Isaacs, L. *Angew. Chem., Int. Ed.* **2005**, *44*, 4844−4870. (b) Lee, J. W.; Samal, S.; Selvapalam, N.; Kim, H. J.; Kim, K. *Acc. Chem. Res.* **2003**, *36*, 621−630.

(5) (a) Odell, B.; Reddington, M. V.; Slawin, A. M. Z.; Spencer, N.; Stoddart, J. F.; Williams, D. J. *Angew. Chem., Int. Ed.* **1988**, *27*, 1547−1550. (b) Brown, C. L.; Philp, D.; Stoddart, J. F. *Synlett* **1991**, 462−646. (c) Asakawa, M.; Dehaen, W.; L'abbé, G.; Menzer, S.; Nouwen, J.; Raymo, F. M.; Stoddart, J. F.; Williams, D. J. *J. Org. Chem.* **1996**, *61*, 9591−9595. (d) Doddi, G.; Ercolani, G.; Mencarelli, P.; Piermattei, A. *J. Org. Chem.* **2005**, *70*, 3761−3764.

(6) (a) Cram, D. J. *Science* **1983**, *219*, 1177−1183. (b) Cram, D. J. *Angew. Chem., Int. Ed. Engl.* **1988**, *27*, 1009−1020. (c) Cram, D. J. *Science* **1988**, *240*, 760−767. (d) Cram, D. J.; Cram, J. M. Container Molecules and Their Guests. In *Monographs in Supramolecular Chemistry*; Stoddart, J. F., Ed.; Royal Society of Chemistry: Cambridge, 1994; Vol. 4.

10.1021/ol070170h CCC: $37.00
Published on Web 03/14/2007

molecules. Given this unique optical property, we have performed[10] calculations on an electrochemically controllable RGB (red/green/blue) dye, which is based on a [2]catenane constitution consisting of an interlocked $CBPQT^{4+}$ ring and a crown ether, having three π-electron-rich stations. The color of this three-station[2] catenane changes as a function of the $CBPQT^{4+}$ ring location (Scheme 1) which, in principle, can be controlled by the oxidation of each station in turn.

Scheme 1. Color Change Scheme of the RGB Dye

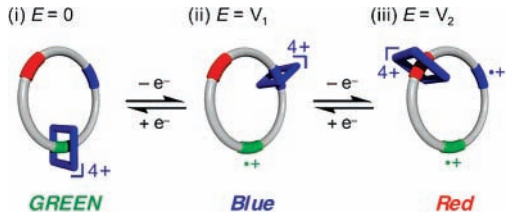

Although for the best part of two decades we have been identifying and examining a range of guest molecules[5a,8,9,11] that can form inclusion complexes with the $CBPQT^{4+}$ ring, the blue color that is suitable for the design of the RGB dye has eluded us.[12] DFT calculations[10] predict that bis-*N*-oligoethyleneglycol-substituted 3,3′-difluorobenzidine should give the required blue color when it forms a complex with the $CBPQT^{4+}$ ring. Here, we describe the synthesis of a new guest compound, bis-*N*-tetraethyleneglycol-substituted 3,3′-difluorobenzidine (**DFBZ-TEG**), for the host, **CBPQT**$^{4+}$, as well as a new [2]rotaxane, **1**·$4PF_6$, using **DFBZ-TEG** as a precursor to its dumbbell. Both the [2]pseudorotaxane and the [2]rotaxane which have their optical (absorption spectrum) and electrochemical properties measured, and thermodynamic parameters deduced, display intense blue colors.

The synthetic routes employed in the synthesis of 3,3′-difluorobenzidine[13] (**DFBZ**), **DFBZ-TEG**, and **1**·$4PF_6$ are summarized in Scheme 2.

Scheme 2. Synthesis of the Blue-colored [2]Rotaxane

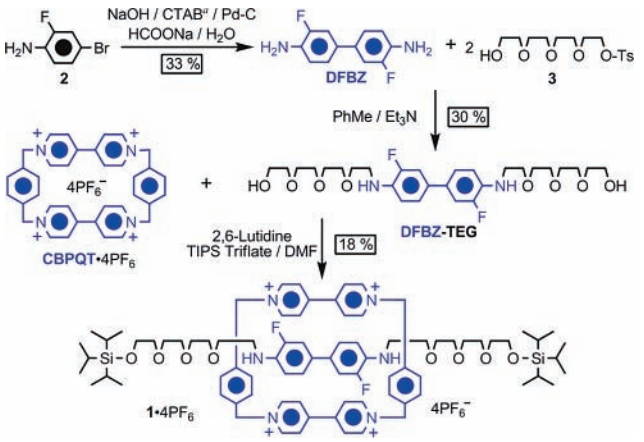

[a] CTAB: Cethyltrimethylammonium bromide.

DFBZ was prepared, starting from 4-bromo-2-fluoroaniline (**2**), in 33% yield using a modification of a procedure already reported in the literature:[13b] the reaction also afforded 3-monofluorobenzidine (15%) and benzidine (**BZ**) itself (10%). **DFBZ** was obtained as a pure compound, free from these byproducts, after column chromatography (SiO_2: MeOH/(2 M) NH_4Cl (aq)/$MeNO_2$, 5:4:1).

DFBZ-TEG was prepared by alkylation (NEt_3/PhMe) of the two amino groups in **DFBZ** with the monotosylate **3** of tetraethyleneglycol.[11,14] Because the reactivity of these amino groups is lower than in **BZ**—presumably on account of both the steric and electronic influences of the fluorine substituents in the 3,3′-positions—the yield of **DFBZ-TEG** was only 30%. When **CBPQT**·$4PF_6$—a white powder—was added to a colorless solution of **DFBZ-TEG** in MeCN, the color of the solution turned blue immediately, indicating the formation of the [2]pseudorotaxane. The [2]rotaxane **1**·$4PF_6$ was isolated in 18% yield as a result of capping[11,15] the terminal hydroxyl groups of this [2]pseudorotaxane with TIPS triflate in DMF laced with 2,6-lutidine.

(7) (a) Ashton, P. R.; Goodnow, T. T.; Kaifer, A. E.; Reddington, M. V.; Slawin, A. M. Z.; Spencer, N.; Stoddart, J. F.; Vicent, C.; Williams, D. J. *Angew. Chem., Int. Ed.* **1989**, *28*, 1394−1395. (b) Bissell, R. A.; Córdova, E.; Kaifer, A. E.; Stoddart, J. F. *Nature* **1994**, *369*, 133−137. (c) Asakawa, M.; Ashton, P. R.; Balzani, V.; Credi, A.; Hamers, C.; Mattersteig, G.; Montalti, M.; Shipway, A. N.; Spencer, N.; Stoddart, J. F.; Tolley, M. S.; Venturi, M.; White, J. P.; Williams, D. J. *Angew. Chem., Int. Ed.* **1998**, *37*, 333−337. (d) Tseng, H.-R.; Vignon, S. A.; Celestre, P. C.; Perkins, J.; Jeppesen, J. O.; Fabio, A. D.; Ballardini, R.; Gandolfi, M. T.; Venturi, M.; Balzani, V.; Stoddart, J. F. *Chem.−Eur. J.* **2004**, *10*, 155−172. (e) Jeppesen, J. O.; Nygaard, S.; Vignon, S. A.; Stoddart, J. F. *Eur. J. Org. Chem.* **2005**, 196−220.

(8) (a) Ashton, P. R.; Gómez-López, M.; Iqbal, S.; Preece, J. A.; Stoddart, J. F. *Tetrahedron Lett.* **1997**, *38*, 3635−3638. (b) Wolf, R.; Asakawa, M.; Ashton, P. R.; Gómez-López, M.; Hamers, C.; Menzer, S.; Parsons, I. W.; Spencer, N.; Stoddart, J. F.; Tolley, M. S.; Williams, D. J. *Angew. Chem., Int. Ed.* **1998**, *37*, 975−978. (c) Steuerman, D. W.; Tseng, H.-R.; Peters, A. J.; Flood, A. H.; Jeppesen, J. O.; Nielsen, K. A.; Stoddart, J. F.; Heath, J. R. *Angew. Chem., Int. Ed.* **2004**, *43*, 6484−6491. (d) Liu, Y.; Flood, A. H.; Stoddart, J. F. *J. Am. Chem. Soc.* **2004**, *126*, 9150−9151.

(9) (a) Philp, D.; Slawin, A. M. Z.; Spencer, N.; Stoddart, J. F.; Williams, D. J. *J. Chem. Soc., Chem. Commun.* **1991**, 1584−1586. (b) Asakawa, M.; Ashton, P. R.; Balzani, V.; Credi, A.; Mattersteig, G.; Matthews, O. A.; Montalti, M.; Spencer, N.; Stoddart, J. F.; Venturi, M. *Chem.−Eur. J.* **1997**, *3*, 1992−1996. (c) Ashton, P. R.; Ballardini, R.; Balzani, V.; Boyd, S. E.; Credi, A.; Gandolfi, M. T.; Gómez-López, M.; Iqbal, S.; Philp, D.; Preece, J. A.; Prodi, L.; Ricketts, H. G.; Stoddart, J. F.; Tolley, M. S.; Venturi, M.; White, A. J. P.; Williams, D. J. *Chem.−Eur. J.* **1997**, *3*, 152−170. (d) Balzani, V.; Credi, A.; Mattersteig, G.; Matthews, O. A.; Raymo, F. M.; Stoddart, J. F.; Venturi, M.; White, A. J. P.; Williams, D. J. *J. Org. Chem.* **2000**, *65*, 1924−1936.

(10) Deng, W.-Q.; Flood, A. H.; Stoddart, J. F.; Goddard, W. A., III. *J. Am. Chem. Soc.* **2005**, *127*, 15994−15995.

(11) Córdova, E.; Bissell, R. A.; Spencer, N.; Ashton, P. R.; Stoddart, J. F.; Kaifer, A. E. *J. Org. Chem.* **1993**, *58*, 6550−6552.

(12) The color of the benzidine complex with **CBPQT**·$4PF_6$ is blue. However, the color of the complex with the bis-*N*-ethyleneglycol-substituted benzidine derivative is greenish blue.

(13) (a) Olah, G.; Pavlath, A.; Kuhn, I. *Acta Chim. Acad. Sci. Hung.* **1955**, *7*, 71−84. (b) Bamfield, P.; Quan, P. M. *Synthesis* **1978**, 537−538.

(14) Ikeda, T.; Saha, S.; Aprahamian, I.; Leung, K. C.-F.; Williams, A.; Deng, W.-Q.; Flood, A. H.; Goddard, W. A., III; Stoddart, J. F. *Chem. Asian J.* **2007**, *2*, 76−93.

(15) Anelli, P.-L.; Ashton, P. R.; Ballardini, R.; Balzani, V.; Delgado, M.; Gandolfi, M. T.; Goodnow, T. T.; Kaifer, A. E.; Philp, D.; Pietraszkiewicz, M.; Prodi, L.; Reddington, M. V.; Slawin, A. M. Z.; Spencer, N.; Stoddart, J. F.; Vicent, C.; Williams, D. J. *J. Am. Chem. Soc.* **1992**, *114*, 193−218.

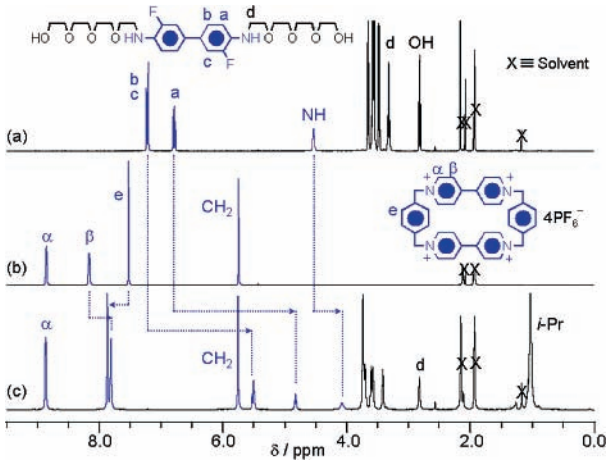

Figure 1. ^{1}H NMR spectra (500 MHz, CD_3CN, rt) of (a) **DFBZ-TEG**, (b) **CBPQT**·4PF_6, and (c) the blue-colored rotaxane **1**·4PF_6.

Figure 1 portrays the ^{1}H NMR spectra of the blue-colored [2]rotaxane **1**·4PF_6 (Figure 1c) and its precursors **DFBZ-TEG** (Figure 1a) and **CBPQT**·4PF_6 (Figure 1b). The signals for the aromatic protons on the rod section of the dumbbell component, i.e., protons a−c, NH, and d, are shifted to a much higher field in the [2]rotaxane **1**·4PF_6, where the $CBPQT^{4+}$ ring expresses its well-known shielding effect on guest protons situated within its cavity. Of the protons associated with the $CBPQT^{4+}$ ring, the chemical shifts for the α and CH_2 protons are almost identical (cf. Figures 1b and 1c), whereas those of the β and e protons are shifted to higher and lower fields, respectively. These observations suggest strongly that the plane of the aromatic ring in **DFBZ** is parallel and perpendicular, respectively, with the bipyridinium and the paraphenylene aromatic rings present in **CBPQT**$^{4+}$, a co-conformation which is consistent with the DFT calculated[10] one.

Table 1. Thermodynamic Parameters for the Inclusion Complexes Formed with **CBPQT**·4PF_6 as a Host in MeCN at 25 °C (Details in Supporting Information)

guest	ΔH (kJ mol^{-1})	$T\Delta S$ (kJ mol^{-1})	ΔG (kJ mol^{-1})	K_a (M^{-1})
DFBZ	−59.0 ± 3.5	−48.4	−10.4	68.3 ± 4.7
DFBZ-TEG	−51.6 ± 0.3	−37.3	−14.2	312 ± 2.5

Table 1 summarizes the thermodynamic parameters for the 1:1 complexes formed between **CBPQT**·4PF_6 as the host and the guests **DFBZ** and **DFBZ-TEG**. The binding constants or K_a values (see Figure S1 in Supporting Information) confirm that the introduction of tetraethyleneglycol chains leads to an increase in the K_a value. Nonetheless, the binding constant does not increase as drastically as when the cores of the guests are tetrathiafulvalene or 1,5-dioxynaphthalene.[16] The trend in K_a values on going from **DFBZ** to **DFBZ-TEG** is consistent with what has been observed previously[11] for biphenol derivatives. Also, it should be noted that the K_a value involving **DFBZ-TEG** as a guest is much smaller than that for the bis-*N*-tetraethyleneglycol-substituted benzidine[17] (**BZ-TEG**), presumably because of the detrimental effect the fluorine atoms have, both electronically and sterically, on the binding of a **BZ** unit inside a **CBPQT**$^{4+}$ host.

UV−visible (UV−vis) absorption spectra of 1:1 mixtures of (a) **DFBZ** and **CBPQT**·4PF_6 and (b) **DFBZ-TEG** and **CBPQT**·4PF_6 and the spectrum of (c) the blue-colored [2]rotaxane, **1**·4PF_6, are illustrated in Figure 2.

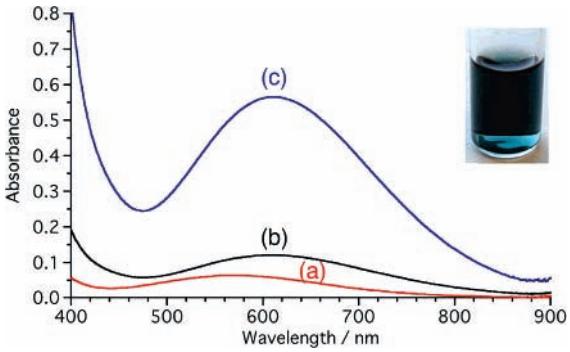

Figure 2. UV−vis absorption spectra (rt, MeCN, 1 mM) of (a) a 1:1 mixture of **DFBZ** and **CBPQT**·4PF_6, (b) a 1:1 mixture of **DFBZ-TEG** and **CBPQT**·4PF_6, and (c) the blue-colored [2]rotaxane **1**·4PF_6. A photograph of the blue-colored [2]rotaxane solution is shown in the inset.

The small K_a values for the [2]pseudorotaxane involving **DFBZ** and **DFBZ-TEG** result in much lower CT absorption intensities (Figures 2a and 2b) compared with that (Figure 2c) of the [2]rotaxane **1**·4PF_6. The introduction of tetraethyleneglycol chains results in a change of the maximum absorption wavelength (λ_{max}) from 570 to 610 nm, indicating that the HOMO energy level of **DFBZ** changes as a direct result of the alkylation of the amino groups.[10,18] The color of the **DFBZ**-based complex in solution can be categorized as purple, rather than as blue. On the other hand, the λ_{max} of 610 nm for the blue-colored **DFBZ-TEG**-based complex and the [2]rotaxane **1**·4PF_6 ($\epsilon = 1.7 \times 10^2$ M^{-1} cm^{-1}) is close to that (601 nm) predicted[10] by DFT calculations.

The electrochemical properties of **DFBZ**, **DFBZ-TEG**, and the blue-colored[2] rotaxane **1**·4PF_6 were analyzed by cyclic voltammetry (CV) (Figure 3) and by differential pulse voltammetry (DPV). See also Figures S2 and S3 in the Supporting Information. The guest compounds (**DFBZ** and **DFBZ-TEG**) show (Figures 3a and 3b, respectively) two

(16) Choi, J. W.; Flood, A. H.; Steuerman, D. W.; Nygaard, S.; Braunschweig, A. B.; Moonen, N. N. P.; Laursen, B. W.; Luo, Y.; DeIonno, E.; Peters, A. J.; Jeppesen, J. O.; Xu, K.; Stoddart, J. F.; Heath, J. R. *Chem.−Eur. J.* **2006**, *12*, 261−279.

(17) The binding constant between **BZ-TEG** and **CBPQT**·4PF_6 is 1910 M^{-1}. See ref 14.

(18) Córdova, E.; Bissell, R. A.; Kaifer, A. E. *J. Org. Chem.* **1995**, *60*, 1033−1038.

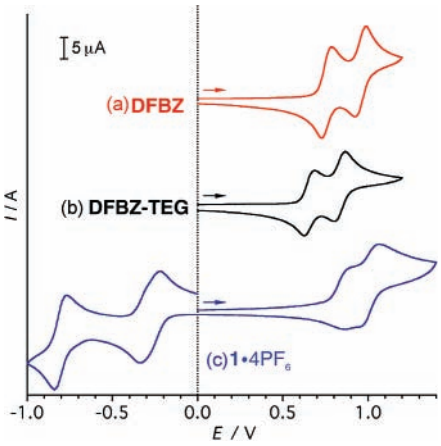

Figure 3. Cyclic voltammetry traces of (a) **DFBZ**, (b) **DFBZ-TEG**, and (c) **1**·4PF_6. The cyclic voltammograms were recorded at 200 mV s^{-1} in argon-purged MeCN at rt. The concentrations of the samples and the supporting electrolyte **TBA**·PF_6 were 0.5 mM and 0.1 M, respectively.

reversible one-electron redox processes. The half-wave potentials ($E_{1/2}$) are summarized in Table 2. The redox potentials of **DFBZ** are higher than those of **DFBZ-TEG**, which is consistent with UV−vis results. The shape of the CV trace in the oxidation region, especially in the cathodic scan, is distorted for **1**·4PF_6. It can be assumed that the flexible tetraethyleneglycol linker enables the $CBPQT^{4+}$ ring to move freely around the **DFBZ** station, a situation which results in the broadening of the redox CV peaks. DPV analysis (Figure S2 in the Supporting Information), however, clearly shows two distinct peaks, which give the exact $E_{1/2}$ values.

Table 2. Half-Wave Potentials ($E_{1/2}$ vs SCE in V) for **DFBZ**, **DFBZ-TEG**, **CBPQT**·4PF_6, and the Blue-Colored [2]Rotaxane **1**·4PF_6[a]

	oxidation	reduction
DFBZ	+0.76, +0.95	
DFBZ-TEG	+0.65, +0.83	
CBPQT·4PF_6		−0.29, −0.72
1·4PF_6	+0.85, +1.02	−0.29, −0.81

[a] Argon purged MeCN, 0.1 M **TBA**·PF_6, 200 mV s^{-1}.

In highly constrained [2]rotaxanes,[18,19] the $E_{1/2}$ value for the second redox process shifts more significantly than the first one because the tetracationic $CBPQT^{4+}$ ring strongly hinders the generation of the dication in the limited available space. In **1**·4PF_6, the first and second $E_{1/2}$ values shift almost in the same magnitude compared with **DFBZ-TEG**: the potential shifts for the first and second oxidations are +0.20 and +0.19 V, respectively. This observation implies that the $CBPQT^{4+}$ ring is slightly translocated from the **DFBZ** station in the direction of the tetraethyleneglycol spacer on account of Coloumbic repulsion after the first oxidation. Because the tetraethyleneglycol is short, the presence of the $CBPQT^{4+}$ ring near the **DFBZ** station still exerts influence on the second redox potential.

Two reversible two-electron redox processes were observed for the $CBPQT^{4+}$ ring in the reduction region ($E < 0$). The first two-electron reduction peak is broad. This broadening is clearly recognizable (Figure S3 in Supporting Information) in the DPV analysis. The broadening arises from the overlap of two peaks as a result of the CT interactions, which mix the **DFBZ** HOMO and the bipyridinium LUMOs together.[19,8] The second two-electron reduction peak does not show broadening,[20] suggesting that the $CBPQT^{2+}$ ring has translocated to one of the tetraethyleneglycol spacers because of weak CT interactions.[9b,d]

In conclusion, we have designed, synthesized, and characterized **DFBZ-TEG** and the [2]rotaxane consisting of **DFBZ-TEG** and **CBPQT**$^{4+}$. We confirmed the blue color of the CT absorption band between **DFBZ-TEG** and **CBPQT**·4PF_6. The acquired data (Table 3) on model compounds (Figure S4 in the Supporting Information)—binding constants, absorption spectra, and electrochemical properties—indicate that the design of an RGB dye using the discussed donor−acceptor motif is attainable.

Table 3. Physicochemical Properties of the Three Model Guests for the RGB Dye

	binding constant K_a M^{-1}	first $E_{1/2}$ vs SCE in V	λ_{max} of CT band nm	
TTF-TEG[a,20]	416,000	+0.36	835	(green)
DFBZ-TEG	300	+0.65	610	(blue)
DNP-C5DEG[a,20]	100	+1.16	525	(red)

[a] The structural formulas are shown in Figure S4 in the Supporting Information.

Acknowledgment. This work was supported by the Microelectronics Advanced Research Corporation (MARCO) and its focus center on Functional Engineered NanoArchitectonics (FENA), the Defense Advanced Research Projects Agency (DARPA), and the Center for Nanoscale Innovative Defense (CNID).

Supporting Information Available: Experimental details, spectroscopic characterization data for all new compounds, DPV analysis results, isothermal titration microcalorimetry results, and the structures of the model guests. This material is available free of charge via the Internet at http://pubs.acs.org.

OL070170H

(19) Flood, A. H.; Nygaard, S.; Laursen, B. W.; Jeppesen, J. O.; Stoddart, J. F. *Org. Lett.* **2006**, *8*, 2205−2208.

(20) In highly-constrained [2]rotaxanes, the second two-electron reduction peak of the $CBPQT^{4+}$ ring also exhibits splitting of the second two-electron reduction peak. See ref. 19.